A Measured Rasorber with Two Absorptive Bands

Weiwei WU, Kaibo CUI, Hongshu LU, Tianzhen MENG, Naichang YUAN*

Coll. of Electronic Science and Engineering, National Univ. of Defense Technology, Changsha, Hunan, 410073, China

978131089@qq.com, 764608294@qq.com*

Submitted December 16, 2016 / Accepted May 22, 2017

Abstract. *In this paper, a novel rasorber with both Frequency Selective Surface and absorptive periodical structure is developed. This rasorber works as a radome and an absorber. Firstly, the design procedure of the unit cell of this rasorber is explained. Then, the characteristics of the manufactured rasorber are measured. The characteristics include the transmission/reflection coefficients of the rasorber, the radiation properties of the horn antenna covered by the novel rasorber and the scattering features of this rasorber. In the passband, the gain of the antenna with our rasorber radome is only 1~2 dB lower than the one of the horn antenna without any radome. Furthermore, the radome has little effect on the radiation patterns of the horn antenna. In the absorptive bands of the rasorber, the electric level of the scattered electromagnetic wave from the rasorber can be 16.5 dB lower than the one from a metallic plane with the same size as the rasorber. The feature proves that this rasorber can be a good candidate in the stealth radar radome area.*

Keywords

Rasorber, radome, absorber, FSS, antenna, RCS reduction

1. Introduction

Each antenna or antenna array in a radar or communication system needs a radome. Recently, besides physical protection, more electromagnetic protection functions are developed and added to the radome. The radomes loaded with Frequency Selective Surface (FSS) are one branch of the research mainstream [1–4]. These radomes reflect at some frequencies and are electromagnetic transparent at other ones like spatial filters. So, the radome-antenna structures are named filtennas [5–7]. These filtennas show good performance in passband and effective rejection to the outband signals. Another branch is the investigation on rasorbers [8–16]. These rasorbers are transparent at some frequencies and absorptive in certain frequency bands.

In our paper, we propose a two-layer rasorber. It has one passband and two absorptive bands. These two absorptive bands are separated by the passband. The transmission/reflection coefficients of the rasorber are simulated and tested firstly. Then it is applied to horn antennas to measure the radiation performance of the rasorber-antenna. Finally, the scattering feature of this rasorber is studied.

2. Design Procedure

Based on the principle of the Salisbury screen [8, 17, 18], a resistive layer and a perfectly conducting ground plane layer are applied to realize the absorption function of the rasorber. A resistive ring is dedicated to the resistive layer of our unit cell. To make the rasorber obtaining bandpass feature, the ground plane is elaborately changed into a periodical slotted ground plane with capacitive and inductive loading. In the filter design, the ring resonator is a good choice to generate a pair of degenerate modes that have the same resonant frequencies but orthogonal field distributions. It resonates at its fundamental frequency f_0 when $2\pi r \approx \lambda_0$ [19]. Because of these degenerate modes, the ring resonator is insensitive to the polarization of the incoming wave. r is the median radius of the ring. It is utilized here to load the slotted ground plane. A metallic pad is inserted into the ring to lower the insertion loss within the pass band. Even with this effort, the insertion loss of the ring-pad FSS unit cell is still high. To achieve low insertion loss in the passband and wide absorptive bands, a better way is to increase the dimensions of the resistive ring and to combine four ring-pad FSS unit cells to form one combination FSS unit cell of the rasorber. The circular aperture in the center of the combination FSS unit cell lowers the insertion loss of the passband further, compared with the combination unit cell without this aperture. The radius of the resistive ring of the combination FSS unit cell is twice as long as the one of a single ring-pad FSS unit cell. The configurations of the ring-pad unit cell and combination unit cell are shown in Fig. 1. High Frequency Simulation Software (HFSS) is applied to do the simulation and optimization.

Two floquet ports (port 1 and port2) of the unit cell model are also shown in Fig. 1(b). After the optimization, the dimensional parameters of the combination FSS unit cell are listed in Tab. 1.

When the incident wave impinges from port 1, the Transmission/Reflection (T/R) coefficients are presented in Fig. 2.

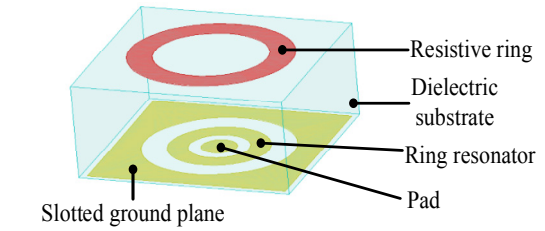

(a) A single ring-pad FSS unit cell.

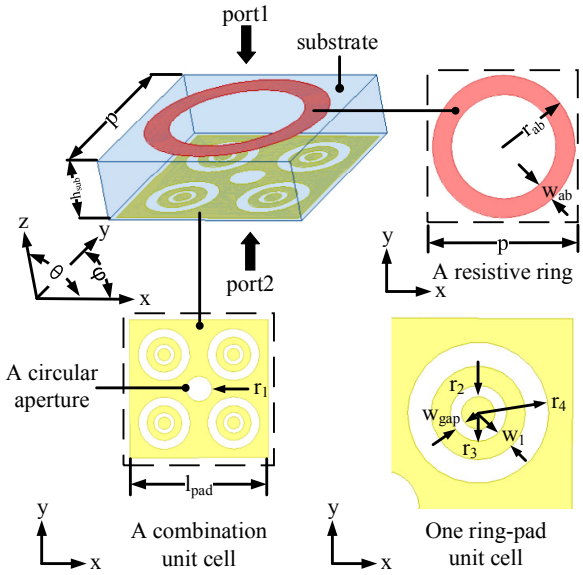

(b) A combination FSS unit cell.

Fig. 1. The configuration of the FSS unit cell.

p = 17 mm	l_{pad} = 16 mm	r_1 = 1.5 mm
r_2 = 0.7 mm	r_3 = 1.2 mm	r_4 = 3 mm
w_1 = 0.8 mm	w_{gap} = 0.5 mm	r_{ab} = 7.5 mm
w_{ab} = 2 mm	h_{sub} = 5 mm	ε_r = 3

Tab. 1. Dimensions of the combination FSS unit cell.

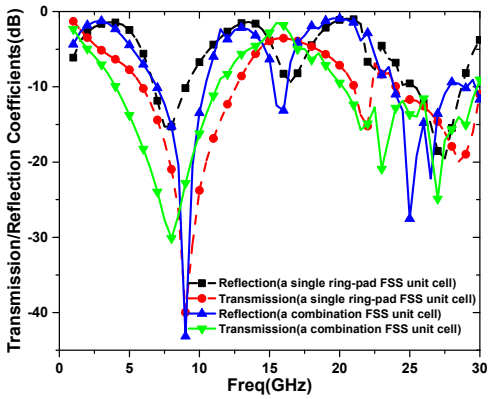

Fig. 2. Transmission/reflection coefficients vs. frequency.

S_{11} represents the reflection coefficient and S_{21} is the transmission coefficient. From Fig. 2, S_{21} of the single ring-pad unit cell is $S_{21} < -3.5$ dB in the whole frequency band. It means that the insertion loss is very big and it cannot be applied to the rasorber. From 15 GHz to 16.5 GHz, S_{21} of the combination FSS unit cell is higher than –3 dB and S_{11} is lower than –10 dB, this is the passband of the rasorber. Otherwise, from 7 GHz to 10.5 GHz, and from 24 GHz to 30 GHz, both S_{11} and S_{21} are lower than –10 dB, these two bands are absorptive bands.

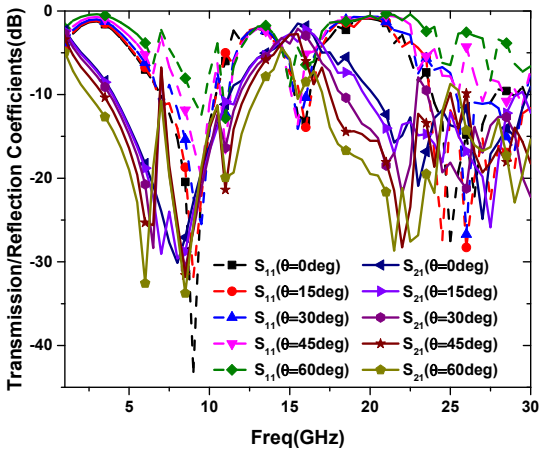

Fig. 3. Transmission/reflection coefficients vs. incident angles.

Since the incidence angle of the impinging incoming wave is unknown for antenna radome to be designed in the real life application, the dependence of absorption and passband frequency intervals on the angle of incidence is plotted in Fig. 3. From this figure, the solid lines represent the transmission coefficients and the dash lines are reflection coefficients. It shows that when the incident angle $\theta \le 45°$, this combination FSS unit cell has both passband and absorptive bands. When $\theta = 60°$ the passband is gone and only a very narrow absorptive band exist around 10 GHz.

3. Experiments of the Radome Performance

The rasorber radome is manufactured and measured, shown in Fig. 4. It has 16 periods in X and Y directions. Its size is 300 × 300 × 5 mm^3. The dielectric substrate is TSM-DS3 from Taconic Company with the dielectric constant and loss tangent given by $\varepsilon_r = 3$ and $\tan\delta = 0.011$, respectively. The resistance of the resistive film is 50 ohm/sq. The circuit board processing technology of the resistive layer and slotted ground plane layer are the same. Both of them are etched on the dielectric substrate.

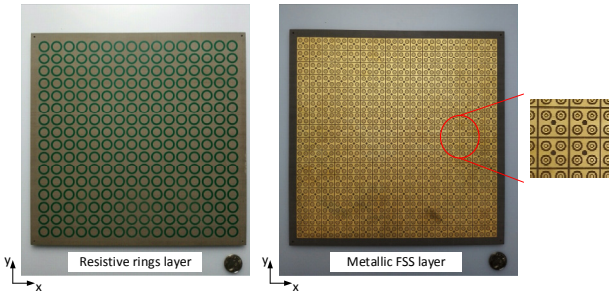

Fig. 4. The manufactured rasorber radome.

3.1 Transmission and Reflection Coefficients

Figure 5 shows the setup for the T/R coefficients measurement in an anechoic chamber. One wideband four arms horn antenna (1~18 GHz) and several standard horn antennas working to 30 GHz are applied to transmit waves. The receiving antennas are standard horn antennas to cover the whole test frequency bands, from 3.9 GHz to 30 GHz. When lowering than 3.9 GHz, the aperture of the horn antenna is bigger than our radome. So the lowest frequency for measurement is 3.9 GHz.

First of all, the transmitting and receiving antennas face each other. The measured $\overline{S}_{21}$ and $\overline{S}_{11}$ are reference values, which are normalized to 0 dB and –30 dB, respectively. Then the rasorber radome is located between these antennas. The measured S_{21} and S_{11} are the transmission/reflection coefficients of the rasorber radome based on $\overline{S}_{21}$ and $\overline{S}_{11}$. The measured curves of the T/R coefficients vs. frequency are shown in Fig. 6. The measured passband ($S_{21} \geq -3$ dB and $S_{11} \leq -10$ dB) is from 14.6 GHz to 18.6 GHz, which is wider than the simulation result. The measured absorptive bands ($S_{21} \leq -10$ dB and $S_{11} \leq -10$ dB) are respectively from 5.6 GHz to 10.8 GHz and from 21.2 GHz to 28.6 GHz. Within higher absorptive band, S_{21} is a little bit bigger than –10 dB from 22.8 GHz to 24.7 GHz. Since the antennas are in the open boundary, which is different from the Master/Slave boundary in the unit cell's simulation in HFSS, the reflection coefficient of the antennas themselves are very small. So even when the radome is located between the transmitting and receiving antennas, the reflection coefficient of the receiving antenna is still very low throughout the whole frequency band, which is different from the simulation results in Fig. 2.

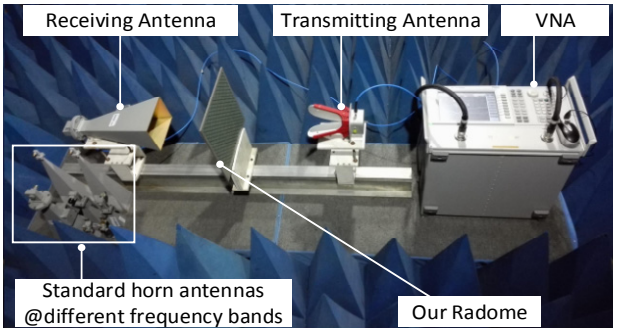

Fig. 5. Test of T/R coefficients of the rasorber radome.

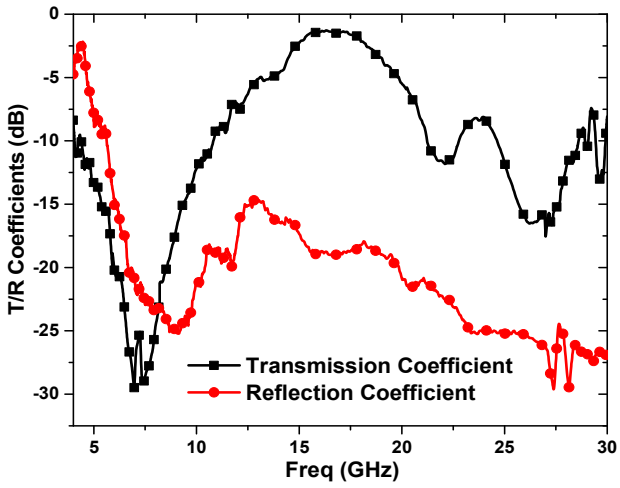

Fig. 6. Measured T/R coefficients of the radome.

3.2 Radiation Characteristic of the Radome-antenna Configuration

Based on the passband of the radome, a horn antenna working from 12 GHz to 18 GHz is utilized. The radiation characteristics of the antenna without our radome ('Only-antenna' curve) and of the antenna with the radome ('Radome-antenna' curve) are measured, depicted in Fig. 7. The distance between the radome and the antenna is 18 mm, which equals the wavelength of the center frequency (16.8 GHz) in passband. From 15.9 GHz to 17.7 GHz, the differences between the gain of the only-antenna and the gain of the radome-antenna are less than 2 dB. Especially, at 16.9 GHz, the gain of the only-antenna is only 1.5 dB higher than the one of the radome-antenna.

Figure 8 shows the normalized E-plane radiation patterns of the radome-antenna and of the only-antenna at

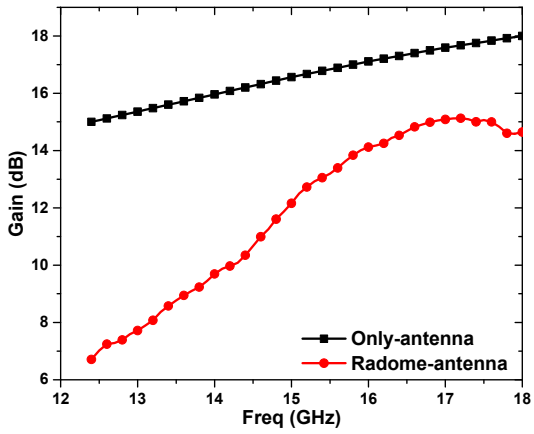

Fig. 7. Gains of the radome-antenna and of the only-antenna vs. frequency.

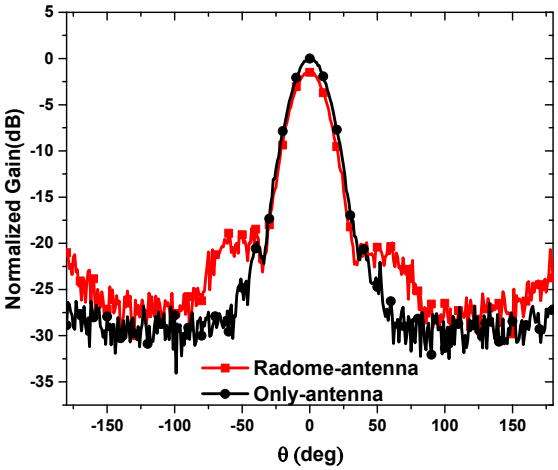

Fig. 8. The normalized E-plane radiation patterns of the radome-antenna and of the only-antenna.

16.9 GHz. When $\theta \in [-40°, 40°]$, the shapes of the main lobes are uniform. Out of this angular range, the side lobe level of the radome-antenna is higher than the one of the only-antenna. It can be concluded that the radome has little effect on the radiation characteristics of the antenna.

3.3 The Scattering Characteristic of the Radome-antenna Configuration

To test the absorption function of this rasorber radome, when the incoming electromagnetic wave emitted by a transmitting antenna impinges on a metallic plane and on our radome respectively, the Electric Level (EL) values of the wave scattered by the metallic plane and by the radome are recorded and compared instead of the monostatic RCS values, shown in Fig. 9. The transmitting antenna and receiving antenna are at the same place. The dimension of the metallic plane is the same as the one of the radome. The resistive rings layer of the radome faces the transmitting/receiving antenna. From Fig. 10, it is illustrated that the electromagnetic wave is absorbed at three frequency bands: from 3.9 GHz to 10.9 GHz, from 12.7 GHz to 19.5 GHz, and from 21.5 GHz to 27.7 GHz. It is apparent that even in the passband, the radome still absorbs the electromagnetic wave. At 8.53 GHz, the EL value of the radome is 16.5 dB lower than the one of the metallic plane. At 16.55 GHz, the EL value of the radome is 11.8 dB lower than the one of the metallic plane. At 25.05 GHz, the EL value of the radome is 13.8 dB lower than the one of the metallic plane.

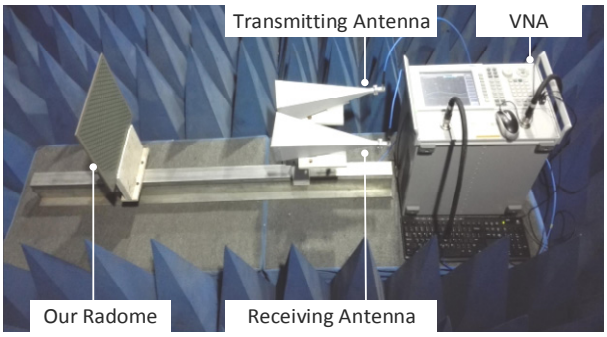

Fig. 9. Measurement setup of the EL value of the scattered wave from the radome and from a metallic plane.

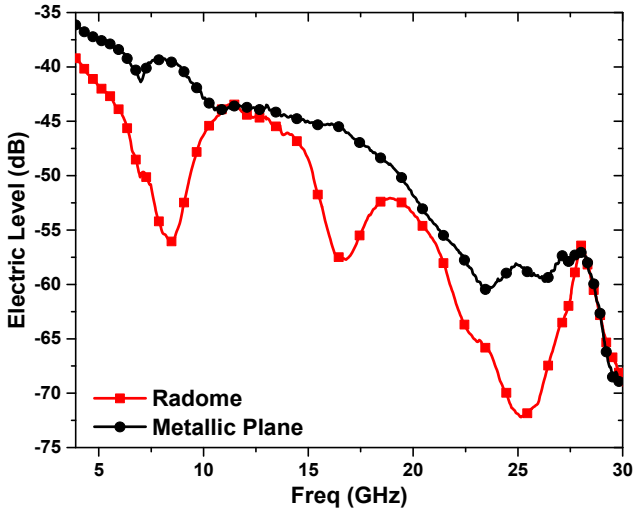

Fig. 10. The measured EL values.

4. Conclusion

A two-layer rasorber radome is developed and measured in this paper. This radome has two absorptive bands separated by one passband. The passband is from 14.6 GHz to 18.6 GHz, and the absorptive bands are from 5.6 GHz to 10.8 GHz and from 21.2 GHz to 28.6 GHz. From 15.9 GHz to 17.7 GHz, the difference between the gain of the radome-antenna and of the only-antenna is less than 2 dB. The radome has little effect on the radiation patterns of the horn antenna. Meanwhile, in the two absorptive bands besides the passband and at the direction of the mainlobe, the electric level value of the scattered wave from the radome can be 16.5 dB and 13.8 dB lower than the one from a metallic plane with the same dimensions as the radome. From this experiment, it is deduced that this rasorber radome can lower the monostatic RCS of a metallic antenna or an antenna array whose dimension is the same as the one of the radome. It is a good choice for the radar stealth radome application.

References

[1] CALOZ, C., ITOB, T. *Electromagnetic Metamaterials Transmission Line Theory and Microwave Applications*. New Jersey (USA): J. Wiley & Sons, 2005. ISBN: 978-0-471-66985-2

[2] HAN, M., HE, M., SUN, H. J., et al. A Frequency Selective Surface radome using a coupled resonator filter. In *2013 IEEE Conference on Microwave Technology & Computational Electromagnetics (ICMTCE)*. Qingdao (China), 2013 DOI: 10.1109/ICMTCE.2013.6812479

[3] ABBASPOUR-TAMIJIANI, A., SARABANDI, K., REBEIZ, G. M. Antenna-filter-antenna arrays as a class of bandpass frequency-selective surfaces. *IEEE Transactions on Microwaves Theory and Technique*, 2004, vol. 52, no. 8, p. 1781–1789. DOI: 10.1109/TMTT.2004.831572

[4] CHEN X., FU, Y, Q., YUAN, N. C. Invisible cloak design with controlled constitutive parameters and arbitrary shaped boundaries through Helmholtz's equation. *Optics Express*, 2009, vol. 17, no. 5, p. 3581–3586. DOI: 10.1364/OE.17.003581

[5] BARBUTO, M., TROTTA, F., TOSCANO, A. Varying the operation bandwidth of metamaterial-inspired filtering modules for horn antennas. *Progress In Electromagnetics Research C*, 2015, vol. 58, p. 61–68. DOI: 10.2528/PIERC15051402

[6] LUO, G. Q., HONG, W., TANG, H. J., et al. Filtenna consisting of horn antenna and substrate integrated waveguide cavity FSS. *IEEE Transactions on Antennas and Propagation*, 2007, vol. 55, no. 1, p. 92–98. DOI: 10.1109/TAP.2006.888459

[7] MA, X. C., HUANG, W., PAN, W., et al. A dual circularly polarized horn antenna in Ku-band based on chiral metamaterial. *IEEE Transactions on Antennas and Propagation*, 2014, vol. 62, no. 4, p. 2307–2311. DOI: 10.1109/TAP.2014.2301841

[8] MUNK, B. A. *Metamaterials: Critique and Alternatives*. New Jersey (USA): J. Wiley & Sons, 2009. ISBN:978-0-470-37704-8

[9] KNOTT, E. F. *Radar Cross Section*. USA: SciTech Publishing, 2004. ISBN: 1-891121-25-1

[10] COSTA, F., MONORCHIO, A. A frequency selective radome with wideband absorbing properties. *IEEE Transactions on Antennas and Propagation*, 2012, vol. 60, no. 6, p. 2740–2747. DOI: 10.1109/TAP.2012.2194640

[11] COSTA, F., MONORCHIO, A., MANARA, G. Analysis and design of ultrathin electromagnetic absorbers comprising resistively loaded high impedance surfaces. *IEEE Transactions on Antennas and Propagation*, 2010, vol. 58, no. 5, p. 1551–1558. DOI:10.1109/TAP.2010.2044329

[12] COSTA, F., MONORCHIO, A., MANARA, G. An equivalent circuit model of frequency selective surfaces embedded within dielectric layers. In *Proceeding of IEEE Antennas and Propagation Society International Symposium*. Charleston (SC, USA), 2009. DOI: 10.1109/APS.2009.5171774

[13] ZHOU, H., QU, S., PENG, W., et al. A novel frequency selective surface loaded with resistance films absorbers. *Acta Physica Sinica,* 2012, vol. 61, no. 10, p. 104201. (in Chinese)

[14] MARTYNYUK, A. E., LOPEZ, M. J. I., MARTYNYUK, N. A. Active frequency-selective surfaces based on loaded ring slot resonators. *Electronics Letters*, 2005, vol. 41, no. 1, p. 2–4. DOI: 10.1049/el:20057774

[15] ZHANG, C. G., ZHANG, Q. Super broad band based on Adaptive Frequency Selective Surface for SAR. In *2nd Asian-Pacific Conference on Synthetic Aperture Radar*, 2009. DOI: 10.1109/APSAR.2009.5374093

[16] ZHOU, H., YANG, L. W., QU, S. B., et al. Experimental demonstration of an absorptive/transmissive FSS with magnetic material. *IEEE Antennas and Wireless Propagation Letters*, 2014, vol. 13, no. 3, p. 114–117. DOI: 10.1109/lawp.2013.2296992

[17] MUNK, B. A. *Frequency Selective Surfaces: Theory and Design*. Hoboken (NJ, USA): John Wiley & Sons, 2000. ISBN: 9780471370475

[18] SALISBURY, W. W. *Absorbent Body for Electromagnetic Waves.* Patent US 2599944 A. 1952.

[19] HONG, J. S., LANCASTER, M. J. *Microstrip Filters for RF Microwave Application*. New Jersey (USA): J. Wiley & Sons, 2001. ISBN: 0-471-22161-9

About the Authors ...

Weiwei WU was born in 1981. She received her M.S. and Ph.D. degree in Electronic Science and Technology from the National University of Defense Technology in 2008 and 2011, respectively. Currently she is a teacher in the College of Electronic Science and Engineering, National University of Defense Technology, Changsha, Hunan, China. Her research interests include array signal processing and antenna design.

Kaibo CUI (*corresponding author) was born in 1990. He received his M.S. degree in Electronic Science and Technology from the National University of Defense Technology in 2013. Currently he is working towards the Ph.D. degree in the College of Electronic Science and Engineering, National University of Defense Technology, Changsha, Hunan, China. His research interests include signal processing and spatial spectrum estimation.

Hongshu LU was born in 1988. He received his M.S. degree in Electronic Science and Technology from the National University of Defense Technology in 2013. Currently he is working towards the Ph.D. degree in the College of Electronic Science and Engineering, National University of Defense Technology, Changsha, Hunan, China. His research interests include passive microwave circuits design and wireless communication.

Tianzhen MENG was born in 1989. She received her M.S. degree in Electronic Science and Technology from the Ordnance Engineering College, National University of Defense Technology in 2014. Currently she is working towards the Ph.D. degree in the College of Electronic Science and Engineering, National University of Defense Technology, Changsha, Hunan, China. Her research interests include antenna design.

Naichang YUAN was born in 1965. He received his M.S. and Ph.D. degree in Electronic Science and Technology from the University Science and Technology of China in 1991 and 1994, respectively. He is currently a professor with the College of Electronic Science and Engineering, National University of Defense Technology, Changsha, Hunan, China. His research interests include array signal processing, signal processing in radar.